**International Journal of Mechanical Engineering and Technology (IJMET)**
Volume 9, Issue 6, June 2018, pp. 1115–1128, Article ID: IJMET_09_06_124
Available online at http://www.iaeme.com/IJMET/issues.asp?JType=IJMET&VType=9&IType=6
ISSN Print: 0976-6340 and ISSN Online: 0976-6359



# MICROSTRUCTURE EVOLUTION OF HIGH MN STEEL THROUGH ART ANNEALING

**Priyadarshan Mahana and Naresh Prasad**
Department of Mechanical Engineering,
National Institute of Technology, Jamshedpur, India

## ABSTRACT

*The various experimental studies are conducted on the medium-Mn steels with Mn content ranged in 3-9% and C content ranged from ultra low carbon to 0.4% were presented. It was shown that long time austenite reverse transformation (ART) annealing of the hardened steels results in an ultrafine ferrite/austenite duplex structure and a substantially improved mechanical property with the product of tensile strength to total elongation about 30-40GPa%. Also, the ART annealing for both short time and long time could be applied to produce the ultrafine duplex structure in the studied steels and the mechanical properties were further improved. The improved mechanical properties of these type of steels were attributed to the ultrafine grains and the large fractioned austenite (30%). Therefore, the stability of austenite is considered as a result of a combination of the dominant role of fine grain austenite size and some contribution of chemical stabilization by Mn and carbon partitioned in the austenite that can be achieved only at specific intercritical temperatures. So, these type of steel presented a premium combination of strength and ductility, $Rm \times A \geq 30GPa\%$. The performances of steel sheets subject to welding, cold forming, cycling loads, and hydrogen fitted well with the existed fabrication technologies for auto steel sheets. It was also found that carbides precipitated during initial annealing stage and gradually dissolved during following annealing process for all annealing temperatures; and interestingly, the fresh martensite was found, indicating that part of the newly forming austenite was unstable and would transform into martensite when quenching Based on the microstructural analysis and the calculation by Thermo-Calc software, it was proposed that the different evolution behaviours of the microstructure during annealing were not only controlled by the thermal kinetics of the austenite, but also affected significantly by the thermal stability of the austenite.*

**Key words:** austenite stability, austenite reverse transformation (ART) annealing, medium-Mn steel, ultra fine grain .

**Cite this Article:** Priyadarshan Mahana and Naresh Prasad, Microstructure Evolution of High Mn Steel Through Art Annealing, *International Journal of Mechanical Engineering and Technology* 9(6), 2018, pp. 1115–1128.
http://www.iaeme.com/IJMET/issues.asp?JType=IJMET&VType=9&IType=6

# 1. INTRODUCTION

With the development of society, the concept of energy saving and ecofriend for vehicles is proposed in recent years. One of the most effective and straightforward way is to reduce the weight of the vehicles. At the same time, it is still very necessary to ensure the safety of the passengers. Therefore, increasingly attention has been paid on the new generation steel which has dual phase structure with very good combination of high strength and high ductility [1, 2]. As both the transformation induced plasticity (TRIP) steels and twinning induced plasticity (TWIP) steels have excellent ductility, it could be expected that increasing the fraction of the relatively stable austenite would effectively improve the ductility [3]. Existence of the metastable retained austenite has been thought to be beneficial as it can improve the ductility of the steels by TRIP or TWIP effects [4 - 9]. The "second generation" of Advanced High Strength Steels (AHSS) is represented by highly alloyed (up to ~17-22 wt.% Mn) and extremely ductile TWIP (Twinning Induced Plasticity) steels having up to 50% elongation at 1000 MPa tensile strength, although they have not found commercial application yet. At the same time, a series of TRIP steels which were relatively cost effective were well developed and widely used in the auto industry. The 3rd generation of AHSS, proposed by Matlock [10], should be less alloyed than TWIP steels, having an intermediate combination of 1000-1200 MPa strength and 20-30 % elongation with supposedly martensite + austenite structure. In most of publications on medium Mn containing steels, the stability of austenite can be attributed to the significant partitioning of Mn between ferrite and austenite during long (hours) holding time in the intercritical temperature range [11-14]. The main heat treatment process designed by us for the medium manganese steels is that the steel will be firstly austenitised at a relatively high temperature (above $Ae_1$) and then followed by quenching and intercritical annealing (between $Ae_1$ and $Ae_3$) to develop ultrafine duplex structure with austenite fraction about 30–40 vol.-%.

In this paper, the medium manganese steel (0.2C– 5Mn) was also processed by the heat treatment mentioned above. The samples were firstly austenitised and then quenched and annealed at different intercritical temperatures with different times. The microstructure evolution during the annealing process was examined by X-ray diffractions (XRD), scanning electron microscopy (SEM) and transmission electron microscopy (TEM). It is well known that the formation and development of metastable austenite were significantly affected by temperature and time. Therefore, in this work, the effects of different annealing temperature with annealing time on the 0.2C–5Mn steel were emphatically studied.

# 2. EXPERIMENTAL PROCEDURES

The steel containing 0.2C–4.75Mn used in the study was prepared by a high frequency induction furnace under the vacuum atmosphere and cast to 20 kg ingots; then the ingots were homogenized at $1250^0$C for 2 h and forged into rods with diameters of 8 mm were austenised at $1050^0$ C for soaking time 30 minutes in trolley furnace and water quenched. In the following heat treatments, the rods were cut into small specimens; and those small specimens were intercritically annealed at different temperatures with different times and finally water quenched to room temperature again. On the basis of the phase diagram shown in Fig. 1, three heat treatments of interest were selected and the heat treatment process was generally schematised in Fig. 2 and the detailed parameters were given in Table 1. Three temperatures are generally located in the lower, middle and upper part of the $\alpha/\gamma$ two-phase region.

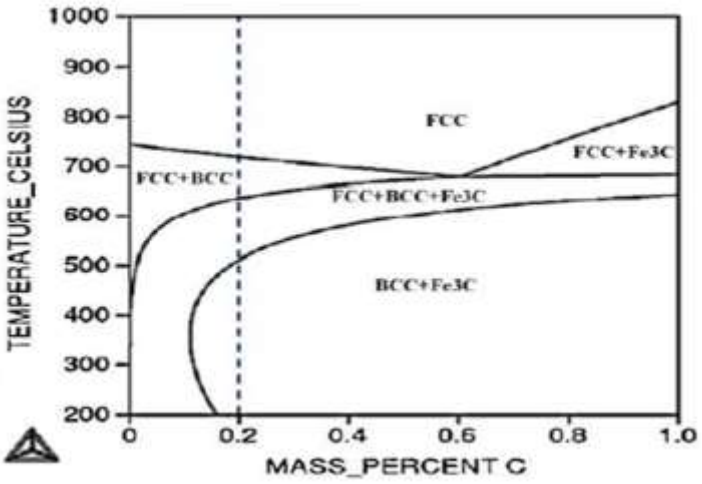


**Figure 1** Phase diagram of designed steel calculated by thermo-calc software.

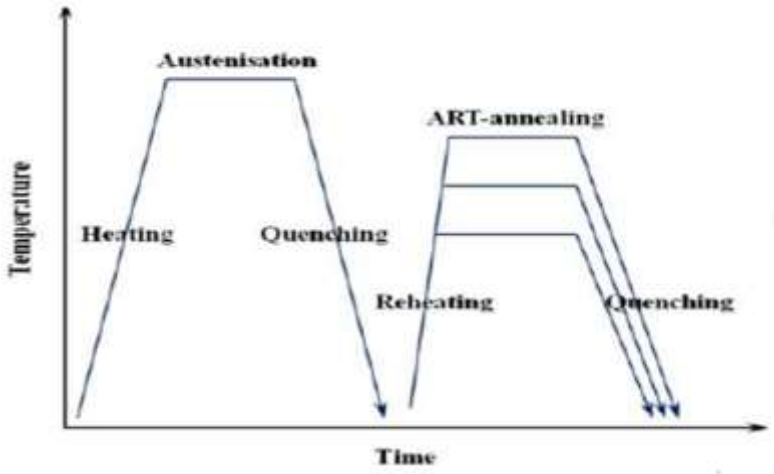


**Figure 2** Scheme of heat treating process.

In this paper, the critical temperatures of $Ae_1$ ($630^0$C) and $Ae_3$ ($720^0$C) and the equilibrium phase diagram of the designed steels shown in Fig. 1 and the equilibrium volume fraction of reversed austenite and its manganese and carbon content were calculated by the commercial thermo-dynamic calculation software Thermo-Calc with its TCFE6 database. Volume fraction of austenite for specimens was estimated by XRD and microstructures of specimens were examined by SEM, and TEM. Manganese contents in ferrite and austenite were measured by energy dispersive spectrometer (TEM– EDS). Samples for XRD and SEM were mechanically grounded, polished and then etched respectively. The XRD with Cu $K_\alpha$ radiation was adopted to measure the volume fraction of retained austenite with the help of Match software. The carbon content of austenite was calculated from the austenite lattice parameters corresponding to their peak positions using the following equation [15].

$$a_\gamma = 3.556 + 0.0453\, x_C + 0.00095 x_{Mn} \quad (1)$$

Where $x_C$ and $x_{Mn}$ (wt%) are carbon content and manganese content in retained austenite.

Table 1. Heat treatment parameters for study in this paper *

| $T_{AU}$ and $t_{au}$ | $T_{an}$ | $t_{an}$ | | | |
|---|---|---|---|---|---|
| $1050^0$ C X 30 min | $620^0$C | 2 min | 10 min | 1 hr | 6 hr 36hr |
| $1050^0$ C X 30 min | $650^0$C | 2 min | 10 min | 1 hr | 6 hr 36hr |
| $1050^0$ C X 30 min | $680^0$C | 2 min | 10 min | 1 hr | 6 hr 36hr |

***** $T_{AU}$: austenisation temperature $T_{au}$: austenisation holding time $T_{an}$: annealing temperature $t_{an}$: annealing time.

## 3. RESULTS

### 3.1. Formation of Austenite during Heat Treatment in (ferrite+austenite) Two-Phase Region

Figure 3 shows the changes in the volume fraction of austenite measured by XRD after water quenched to room temperature from each heat treatment temperature in the two-phase (ferrite + austenite) region at 620, 650 and $680^0$C as a function of the holding time. Such gradual reversion behaviour indicates that it is a diffusional phase transformation process during the intercritical annealing. And the growth of austenite is usually accompanied with the partition of Mn.

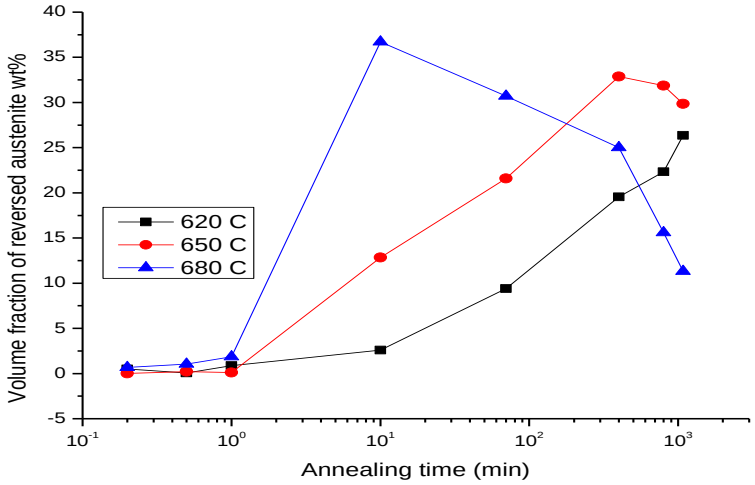


**Figure 3** Changes in volume fraction of austenite after cooling from each heat treatment process in the (ferrite + austenite) two-phase region at 620, 650 and $680^0$C respectively

When the annealing temperature is low ($620^0$C), the amount of retained austenite at room temperature increased solely with time as shown in Fig. 3. While at 650 and $680^0$C (Fig. 3), with increasing annealing temperature, the amount of retained austenite at room temperature firstly increased with time and then decreased. However, the amount of retained austenite for $650^0$C case decreased very slightly, while the amount of retained austenite for $680^0$C case (Fig. 3) decreased sharply and was much lower than that for the $650^0$C case and even lower than that for the $620^0$C case eventually. The maximum volume fractions of retained austenite obtained under these heat treatment conditions were 26.6 vol.-% ($620^0$C), 33.0 vol.-% ($650^0$C) and 36.5 vol. percent ($680^0$C). Figure 4 shows the hardness variation with the changes of annealing temperature and time. At $620^0$C,$650^0$C the hardness decreased solely with annealing time. And at $680^0$C the hardness decreased at first and then increased with increasing annealing time.

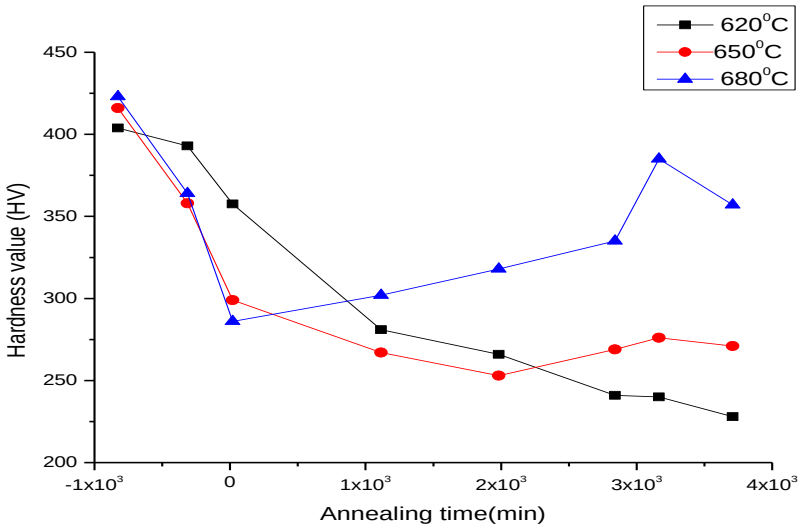


**Figure 4** Hardness changes after cooling from each heat treatment process in (ferrite+ austenite) two phase regions at 620,650 and 680$^0$C respectively.

## 3.2. Observation of Microstructure Evolution

### *3.2.1. Microstructure evolution characterized by SEM*

The microstructure (examined by SEM) for 0.2C–5Mn steel which was austenised at 1000$^0$C for 30 min and followed by water quenching was presented in Fig. 5.

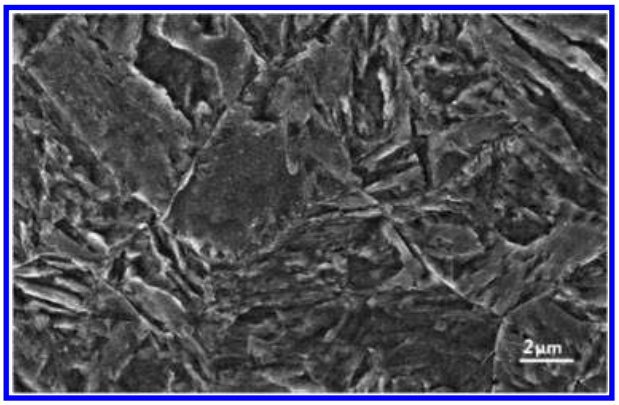


**Figure 5** Microstructure of 0.2C–5Mn steel austenitising at 1050$^0$C for 30 min with water quenching characterized by SEM.

It can be found that the microstructure is full martensite lath structure without carbides or austenite.The microstructure evolution (examined by SEM) of 0.2C–5Mn steel which was intercritically annealed at 620$^0$C after austenisation at 1050$^0$C was shown in Fig. 6. In this intercritical annealing process, the steel was annealed at a temperature located in the lower part of the two-phase region. It can be found that, during the annealing, at the early stage, the carbides precipitated and there were almost no other phases but martensite laths with precipitated carbides. And the amount of carbides increased with increasing annealing time. However, with the duration of annealing (more than 10 min), a solute rich $\gamma$ phase (austenite) formed and developed predominantly at the martensite lath boundaries and remained stable when water quenched to room temperature [16] and the carbides, which precipitated at the early stage gradually, dissolved into the newly forming austenite leading to the decrease of carbides and the formation of duplex lath

structure. And with the dissolving of carbides, the duplex structure became clear. And it can also be found that, although the amount of carbides decreased, it did not totally disappeared eventually. And it is in a very good agreement with the result predicted by the phase diagram as shown in Fig. 1.

The microstructure evolution (examined by SEM) of 0.2C–5Mn steel intercritically annealed at $650^0$C after austenisation at $1050^0$C was shown in Fig. 7. It can also be found that the carbides precipitated at the very early stage (only with a few minutes). And compared with that of the $620^0$C case (Fig. 6*a*), its amount increased. And the whole microstructure also consisted of martensite lath structure matrix and a lot of precipitated carbides. Austenite can hardly be found. And with the increase of annealing time, the carbides also gradually dissolved into the gradually forming austenite and became very little at last.

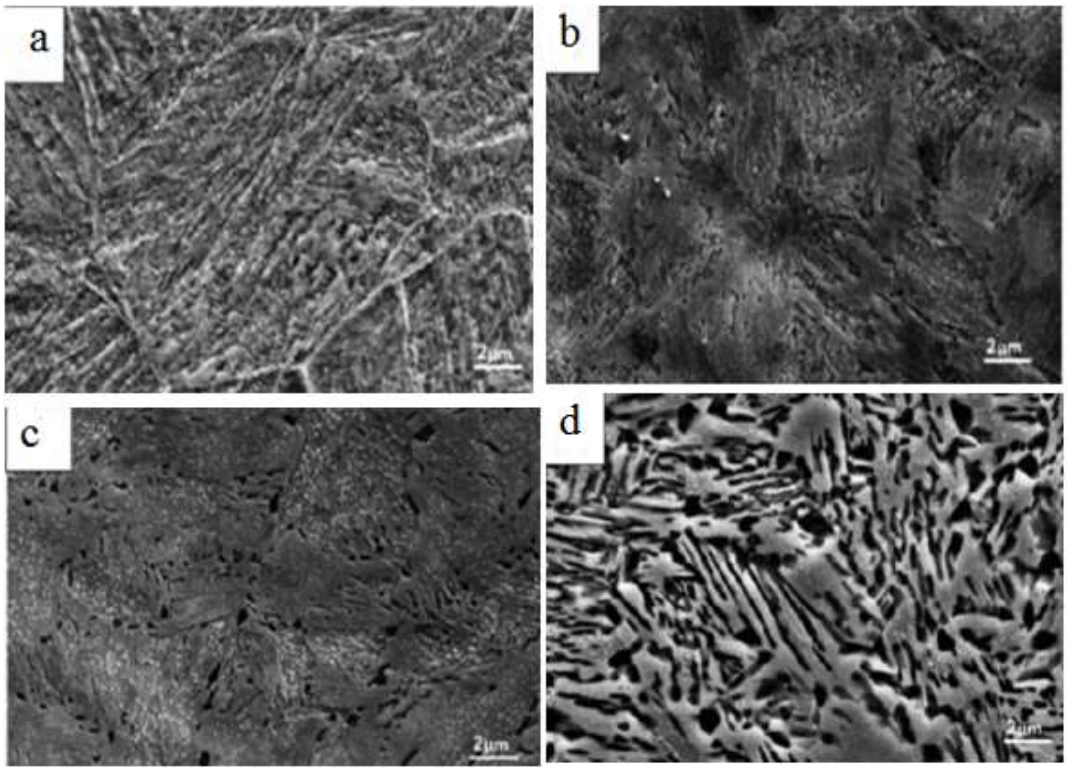


**Figure 6** Microstructure evolution of 0.2C–5Mn steel annealing at $620^0$C for *a* 2 min, *b* 10 min, *c* 1 h, *d* 6 h, characterized by SEM.

The microstructure evolution (examined by SEM) of 0.2C–5Mn steel intercritically annealed at $680^0$C after austenisation at $1050^0$C was shown in Fig. 8. In this intercritical annealing process, the steel was reheated to the temperature located in the upper part of the two phase region which is close to the $Ae_3$ temperature. Therefore, the volume fraction of reversed austenite is very high (Fig. 13). It can be found that the microstructure evolution process is almost the same as the process of $620^0$C (Fig. 6) and $650^0$C (Fig. 7) cases at the initial stage (less than 10 min). The austenite formed preferentially along the martensite lath boundaries and a microstructure of parallel laths of alloy rich austenite and alloy lean tempered martensite (ferrite) gradually formed. A large amount of carbides can also be found and gradually dissolved into the new forming austenite. And with increasing annealing time, the duplex structure became the most clear at 10 min as shown in Fig. 7*d*, which indicated that the amount of austenite reached the

maximum at this temperature with this annealing time. And with longer annealing time, the austenite decreased, which agreed quite well with the result as shown in Fig. 3.

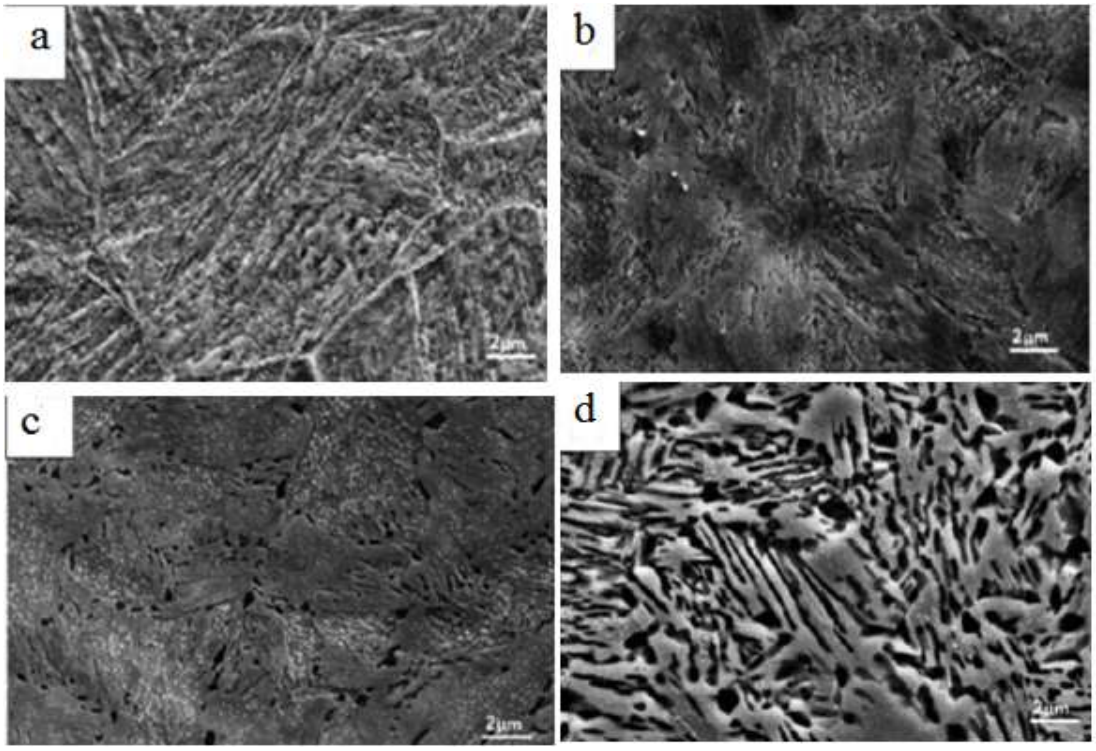


**Figure 7** Microstructure evolution of 0.2C–5Mn steel annealing at $650^0$C for *a* 2 min, *b* 10 min, *c* 1 h, *d* 6 h, characterized by SEM.

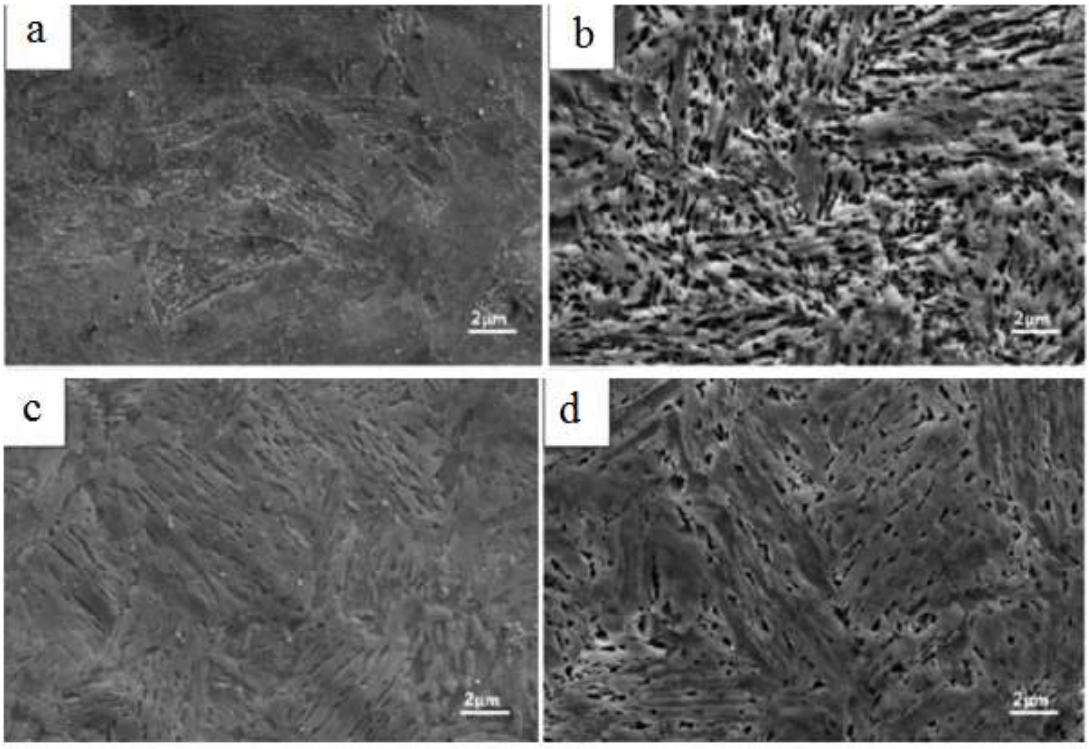


**Figure 8** Microstructure evolution of 0.2C–5Mn steel annealing at $680^0$C for *a* 2 min, *b* 10 min, *c* 1 h, *d* 6 h, characterized by SEM.

### *3.2.2. Microstructure evolution characterized by TEM*

The initial microstructure after the austenisation and water quenching was determined as fully martensitic structure both by SEM and XRD. The analysis of the microstructure after intercritical annealing (Fig. 9) indicated that part of the reversed austenite retransformed into martensite during the water quenching. And the final microstructure presents three phases: retained austenite, ferrite and the fresh martensite.

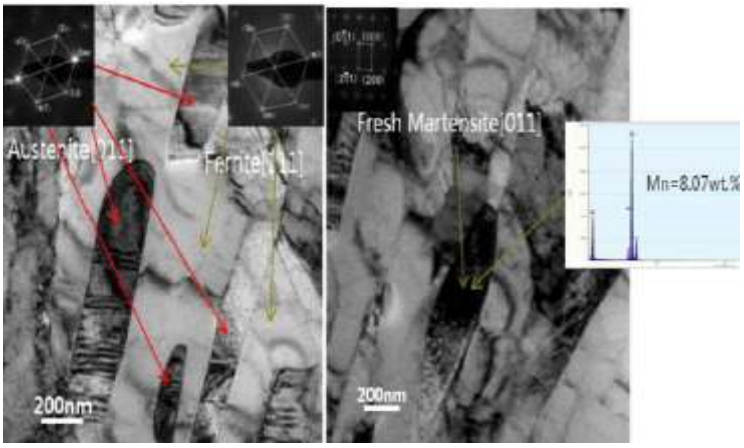


**Figure 9** Microstructure of sample annealed for 36 h at 620$^0$C characterised by TEM images

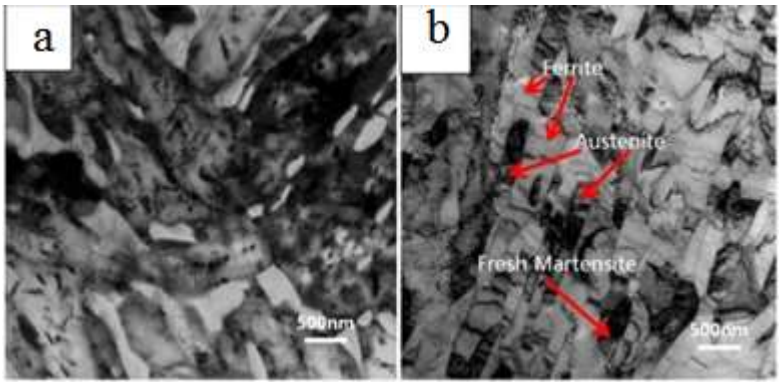


**Figure 10** TEM images showing microstructure evolution in reversion treated specimens at 6200C with a 6 h and b 36 h.

TEM images in Fig. 10 show the microstructure evolution of 0.2C–5Mn steel processed by annealing at 620$^0$C with different times. With increasing annealing time, the duplex structure (Fig. 10 *a* and *b*) became clearer and the amount of austenite increased obviously, while the thickness of austenite lath increased slightly up to about 250 nm, which was still relatively very small. In the 6 h case (Fig. 10*a*), both granular and rod shaped carbides were found and which certified the results shown in Fig. 6. And in the specimen annealed for 36 h (Fig. 10*b*), few carbides can be found and instead, more austenite laths developed between martensitic laths, which may indicate that the austenite laths preferred to nucleate at the martensitic laths interface or the packet boundary rather than at the inside of each martensite lath.

The microstructure evolution of 0.2C–5Mn steel processed by annealing at 650$^0$C with different times was characterized by TEM as shown in Fig. 11. The retained austenite could hardly be found in this nearly full martensite structure. With increasing annealing time, the lamellar duplex structure became clear and the thickness of austenite lath also slightly increased (Fig. 11*a* and *b*). And carbides can hardly be found. In the 6 h

annealed sample, the microstructure consisted of austenite laths, ferrite laths and/or fresh martensite. And the thickness of austenite lath was around 200 nm.

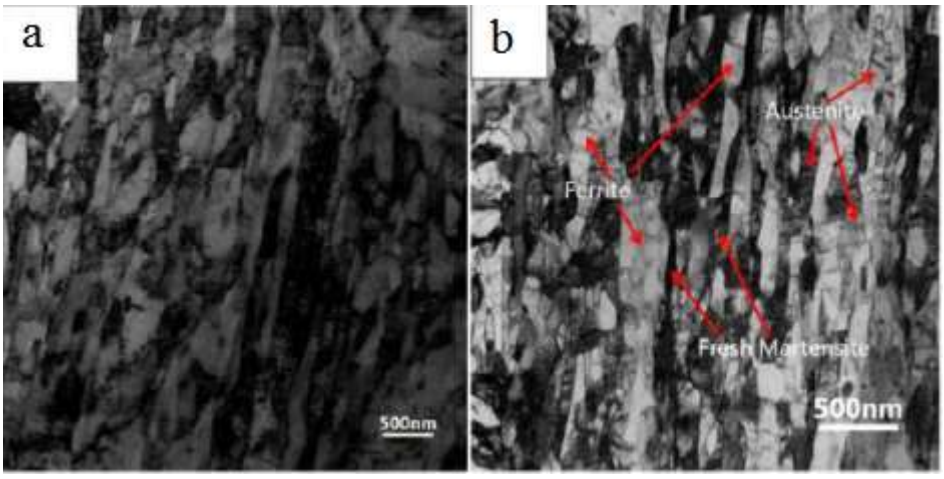


**Figure 11** TEM images showing microstructure evolution in reversion treated specimens at $650^0$C with *a* 1 h and *b* 6h

The microstructure evolution of 0.2C–5Mn steel annealed at $680^0$C with different times was shown in Fig. 12. When annealing time was for 10 minutes, the microstructure was found a clear lamellar duplex structure. Comparing the austenite lath of the 10 min case (around 200 nm shown in Fig. 12*a*) with that of 6 h case (around 400 nm shown in Fig. 12*b*), it can be found that the thickness of austenite lath also increased with increasing annealing time.

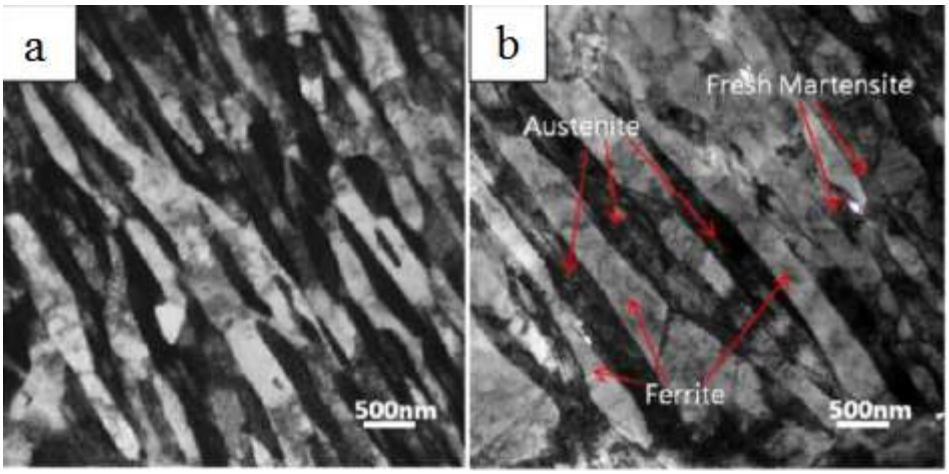


**Figure 12.** TEM images showing microstructure evolution in reversion treated specimens at $680^0$C with *a*10 min and *b* 6 h.

## 4. DISCUSSION

### 4.1. Formation of Austenite during Intercritical Annealing Process

Base on the XRD results (Fig. 3), it is found that, at the very first stage (less than 2 min), there is almost no or very little retained austenite forming during all heat treatment cases. And at the second stage, the volume fraction of austenite increased with increasing holding time in all the cases of heat treatment while decreasing at the third stage in the cases of heat treatment at 650 and $680^0$C. This is generally due to the retransformation

of reversed austenite to martensite [17, 18] (formation of fresh martensite) during the water quenching process.

In order to understand the retransformation behaviours of the intercritically annealed 0.2C–5Mn steel, the equilibrium volume fraction and manganese and carbon contents of reversed austenite were calculated by the commercial thermodynamic calculation software ThermoCalc with its TCFE6 database (Figs. 13–15). From Fig. 13, it can be seen that the volume fraction of reversed austenite gradually increases with increasing holding temperature, and each levels off at around 36.0 and 47.2, and 63.8% at 620, 650 and 680$^0$C respectively.

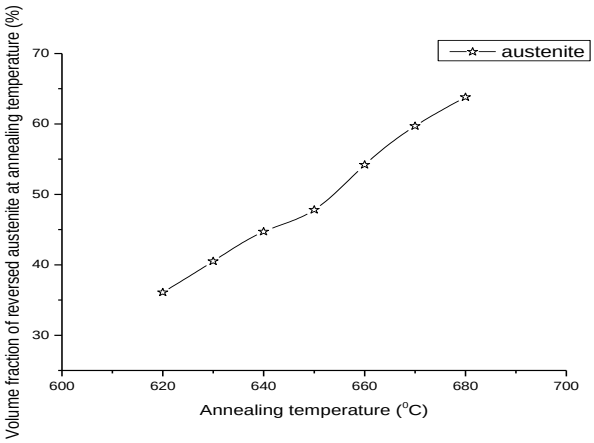


**Figure 13** Equilibrium volume fraction of reversed austenite as function of temperature from thermo-calc software

Figure 14 shows that the manganese (Fig. 14*a*) and carbon (Fig. 14*b*) contents of reversed austenite in 0.2C–5Mn steels grade as a function of temperature and both of them decreased with increasing annealing temperature. And the manganese (Fig. 14*a*) and carbon (Fig. 14*b*) contents were not only predicated by Thermo-Calc but also estimated by TEM–EDS (for 36 h annealing) and XRD (for 36 h annealing).

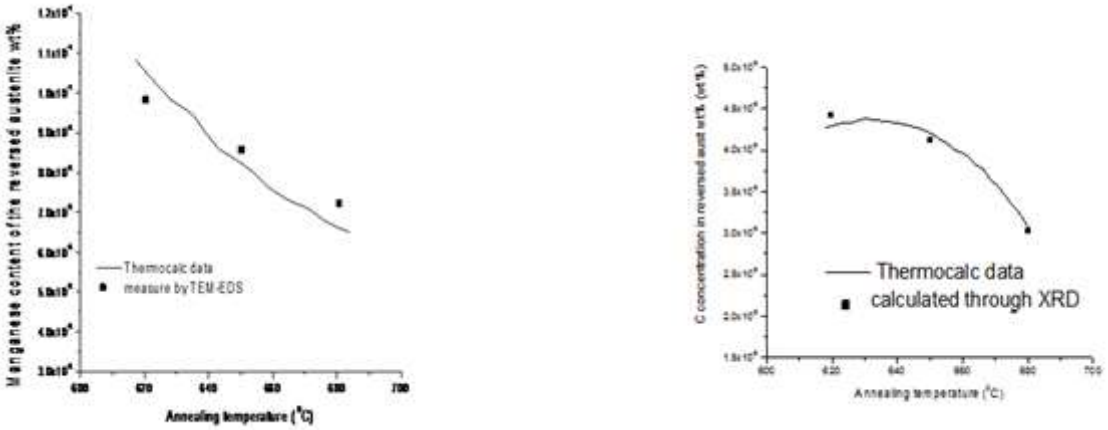


**Figure 14a and 14b.** a. manganese and b Carbon contents of reversed austenite in 0.2C-5Mn steels as function of temperature estimated from TEM-EDS and XRD along with thermo-calc data

From Fig. 15, it can be found that the manganese content of reversed austenite at 680$^0$C grades as a function of time and it decreased with increasing annealing time.

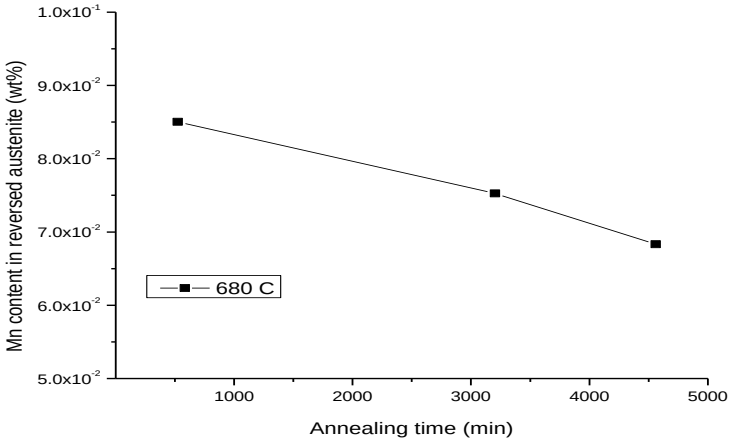


**Figure 15** Manganese in reversed austenite as function of time by TEM-EDS

When the annealing temperature is low ($620^0$C), the quenching stability of the reversed austenite will be good due to the enrichment of austenite stabilised elements (with ~ 10.7wt% Mn and ~ 0.43wt% C as shown in figure 14) in reversed austenite. Therefore it is difficult for the reversed austenite (forming during the annealing process) to retransform to martensite during the cooling. And it is shown in Fig. 3 that the amount of retained austenite (after cooling to room temperature) increases all the time and does not decrease. And with increasing annealing temperature, the volume fraction of reversed austenite arises (Fig. 13), so the average content of the manganese and carbon elements in the reversed austenite will decrease (Fig. 14). As the higher the annealing temperature is, the less the average content of the manganese and carbon elements in the reversed austenite will be. The quenching stability of austenite will decrease with increasing annealing temperature. Therefore, the amount of retained austenite (after quenching to room temperature) will decrease at last. While above the $650^0$C (Fig. 3), the amount of retained austenite at room temperature decreased and the amount of retained austenite for $650^0$C case (Fig. 3) decreased very slightly, which indicated that the quenching stability of reversed austenite at $650^0$C (with $\sim$ 8.35 wt-%Mn and $\sim$ 0.42 wt-%C as shown in Fig. 14) did not decrease very much with longer annealing time. However, the amount of retained austenite for $680^0$C case (Fig. 3) was much lower than that for the $650^0$C case and even lower than that for the $620^0$C case after long time annealing. Therefore, it indicated that the quenching stability of reversed austenite at $680^0$C (with $\sim$ 6.76 wt-%Mn and $\sim$ 0.31 wt-%C as shown in Fig. 14) decreased a lot with longer annealing time as the amount of reversed austenite at $680^0$C increased very much (approaching 63.8 vol.-% as shown in Fig. 13) and the manganese content of reversed austenite decreased a lot as shown in Fig. 15. And water quenching hence resulted in the retransformation of the reversed austenite into fresh martensite [20]. Therefore, the respective maximum volume fractions of retained austenite (after cooling to room temperature) obtained under those heat treatment conditions, which are 26.6 vol.-% ($620^0$C), 33.0 vol.-% ($650^0$C) and 36.5 vol.-% ($680^0$C) as shown in Fig. 3, are less than the volume fractions of reversed austenite (forming during the annealing process), which are 36.0 vol.-% ($620^0$C), 47.2 vol.-% ($650^0$C) and 63.8 vol.-% ($680^0$C) obtained at the same temperature as shown in Fig. 13.

Figure 4 shows the hardness variation with the changes of annealing temperature and time. The decrease in hardness is related to the recovery of martensite and the

increase of retained austenite (Fig. 3). However, the increase in hardness results from the retransformation of the reversed austenite to martensite during the cooling process [19]. With increasing annealing temperature and time, the amount of fresh martensite increased. More reversed austenite retransformed into martensite for the $680^0$C case than for the $650^0$C case, which resulted that the increase in hardness for $680^0$C is larger than that for $650^0$C (Fig. 4).

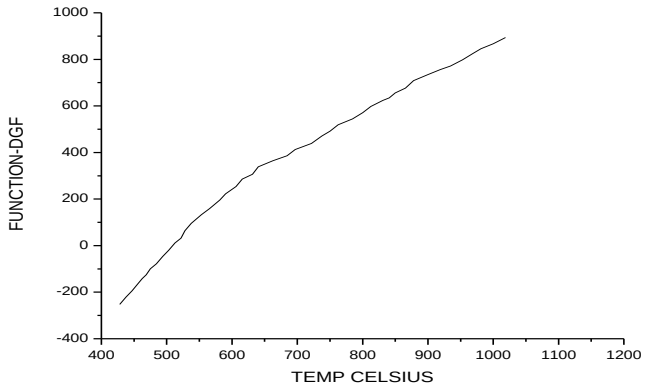


**Figure 16** Driving force for reversed austenite transforming through Thermo-calc

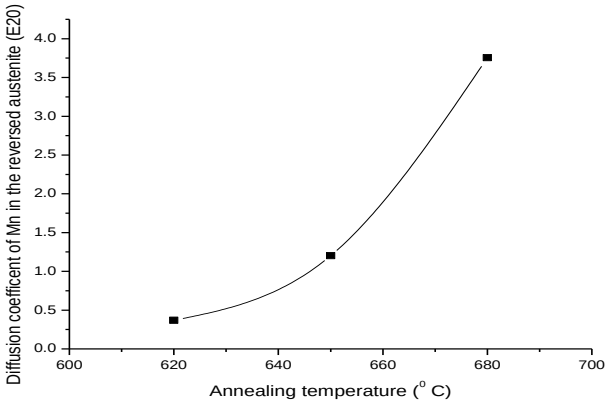


**Figure 17** Diffusion coefficient of Mn in austenite

It can also be found (Fig. 3) that the time needed for the different heat treatment processes to get the maximum volume fractions of retained austenite decreased significantly with increasing annealing temperature. In the $620^0$C case, the time needed for obtaining the maximum volume fraction of retained austenite (～ 26.6 vol.-%) is about or even more than 36 h. While in the $680^0$C case, the time needed for obtaining the maximum volume fraction of retained austenite (～ 36.5 vol.-%) is only about 5–10 min. It may be explained that the driving force (obtained through Thermo-Calc) for reversed austenite transforming and the diffusion coefficient of the manganese in austenite increased with increasing annealing temperature as shown in Figs. 16 and 17 respectively.

## 5. CONCLUSIONS

Intercritical annealing treatments were applied on the 0.2C–5Mn steel. Austenite reverted transformation process was observed during the intercritical annealing. The amount of the retained austenite and the evolution of microstructure at different temperatures with

increasing annealing time were studied. The results were generally summarised as follows:

1. After austenisation at $1050^0$C for 0.5 h and water quenching, a full martensite structure was found in the specimen. During the following annealing process, it gradually transformed into the austenite and ferrite duplex structure. After the quenching, as part of the reversed austenite retransformed into fresh martensite, the final structure became a complex ultrafine structure of retained austenite, ferrite and fresh martensite.

2. The annealing time and temperature are the two key parameters to obtain and control the final compound structure. At the relative lower annealing temperature ($620^0$C close to $Ae_1$ temperature), the austenite volume fraction increased continuously with increasing annealing time. During the $650^0$C annealing process, the austenite volume fraction increased with increasing annealing time firstly, but then slightly decreased. While at the relative higher annealing temperature ($680^0$C close to $Ae_3$ temperature), the austenite volume fraction increased sharply up to the maximum 36.5 vol.-% with only 10 min and then very quickly decreased with increasing annealing time.

3. Under the different heat treatment conditions, the maximum retained austenite volume fractions were obtained about 26.6, 33.0 and 36.5 vol.-% at 620, 650 and $680^0$C respectively.

## REFERENCES


[1] K. Sugimoto, N. Usui, M. Kobayashi and S. Hashimoto "Effects of Volume Fraction and Stability of Retained Austenite on Ductility of TRIP-aided Dual-phase Steels" ISIJ Int., 1992, 32, (12), 1311–1318.

[2] K. Sugimoto, T. Iida, J. Sakaguchi and T. Kashima "Retained Austenite Characteristics and Tensile Properties in a TRIP Type Bainitic Sheet Steel" ISIJ Int., 2000, 40, 902.

[3] A. Arlazarov, M. Goune, O. Bouaziz, A. Hazotte, G. Petitgand and P. Barges "Evolution of microstructure and mechanical properties of medium Mn steels during double annealing" Mater. Sci. Eng. A, 2012, A542, 31–39.

[4] A. K. Srivastava, G. Jha, N. Gope and S. B. Singh "Effect of heat treatment on microstructure and mechanical properties of cold rolled C–Mn–Si TRIP-aided steel" Mater. Charact., 2006, 57, (2), 127–135.

[5] J. Zrnik, O. Stejskal, Z. Novy and P. Hornak "Relationship of microstructure and mechanical properties of TRIP-aided steel processed by press forging" J. Mater. Process. Technol., 2007, 192–193, 367–372.

[6] K. Ahn, D. Yoo, M. H. Seo, S. H. Park and K. Chung "Springback prediction of TWIP automotive sheets" Met. Mater. Int., 2009, 15, (4), 637–647.

[7] K. Chung, K. Ahn, D. H. Yoo, K. H. Chung, M. H. Seo and S. H. Park "Formability of TWIP (twinning induced plasticity) automotive sheets" Int. J. Plast., 2011, 27, (1), 52–81.

[8] S. Allain, J. P. Chateau and O. Bouaziz "A physical model of the twinning-induced plasticity effect in a high manganese austenitic steel" Mater. Sci. Eng. A, 2004, A387, 143–147

[9] O. Bouaziz, S. Allain and C. Scott "Effect of grain and twin boundaries on the hardening mechanisms of twinning-induced plasticity steels" Scr. Mater., 2008, 58, (6), 484–487.

[10] D.K. Matlock and J.G. Speer: Proceeding of The 3rd International Conference on Advanced Structural Steels, Gyeongju, Korea, (2006), p. 774.

[11] R.L. Miller "Ultrafine-grained microstructures and mechanical properties of alloy steels" Metallurgical Transactions, Vol. 3 (1972), p. 905.

[12] T. Furukawa "Dependence of strength–ductility characteristics on thermal history in lowcarbon, 5 wt-%Mn steels" Materials Science and Technology, Vol. 5 (1989), p. 465

[13] H. Huang, O. Matsumura, T. Furukawa "Effects of carbon content on mechanical properties of 5%Mn steels exhibiting transformation induced plasticity" Materials Science and Technology, Vol. 10 (1994), p. 621.

[14] T. Furukawa, H. Huang, O. Matsumura "Retained austenite in low carbon, manganese steel after intercritical heat treatment" Materials Science and Technology, Vol. 10 (1994), p. 964.

[15] M. E. Jimenez, N. H. van Dijk, L. Zhao, J. Sietsma, S. E. Offerman, J. P. Wright and S. van der Zwaag "The effect of aluminium and phosphorus on the stability of individual austenite grains in TRIP steels" Acta Mater. 2009, 57, (2), 533–543.

[16] J. I. Kim, C. K. Syn and J. W.Morris "Microstructural sources of toughness in QLT-Treated 5.5Ni cryogenic steel" Metall. Trans. A, 1983, 14A, 93-103.

[17] N. Nakada, T. Tsuchiyama, S. Takaki and N. Miyano "Temperature Dependence of Austenite Nucleation Behavior from Lath Martensite" ISIJ Int., 2011, 51, (2), 299–304.

[18] P. Wang, S. P. Lu, D. Z. Li, X. H. Kang and Y. Y. Li "Phase Transformation During Intercritical Tempering with High Heating Rate in a Fe-13%Cr-4%Ni-Mo Stainless Steel" Acta Metall. Sin., 2008, 44, (6), 681

[19] E. S. Park, D. K. Yoo, J. H. Sung, C. Y. Kang, J. H. Lee and J. H.

[20] Sung "Formation of reversed austenite during tempering of 14Cr−7Ni−0.3Nb−0.7Mo−0.03C super martensitic stainless steel" Met. Mater. Int., 2004, 10, (6), 521–525.